

Lawrence Berkeley National Laboratory

Recent Work

Title

LIFETIME MEASUREMENTS AT PEP AND PETRA

Permalink

<https://escholarship.org/uc/item/3dw7j8mc>

Author

Goldhaber, G.

Publication Date

1985-10-01

c.2



Lawrence Berkeley Laboratory

UNIVERSITY OF CALIFORNIA

Physics Division

Invited talk presented at the XVI Symposium on
Multiparticle Dynamics, Kiryat-Anavim, Israel,
June 9-14, 1985

LIFETIME MEASUREMENTS AT PEP AND PETRA

G. Goldhaber

October 1985

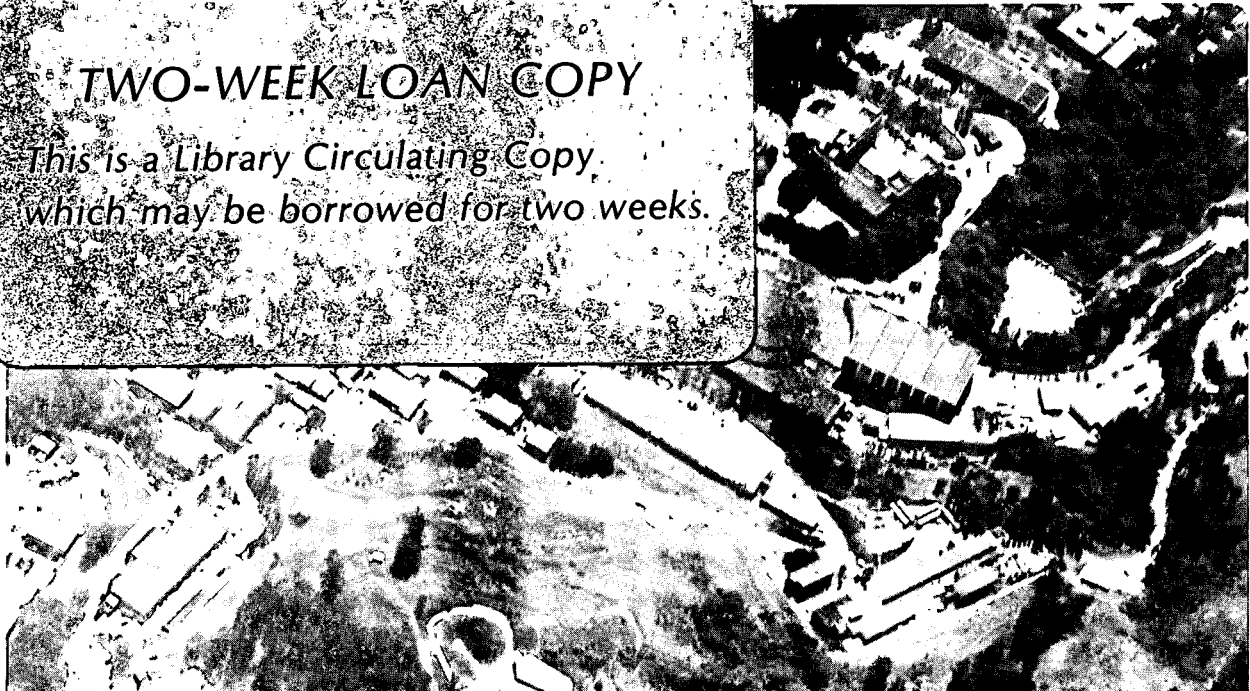
RECEIVED
LAWRENCE
BERKELEY LABORATORY

DEC 18 1985

LIBRARY AND
DOCUMENTS SECTION

TWO-WEEK LOAN COPY

*This is a Library Circulating Copy,
which may be borrowed for two weeks.*



LBL-20445
c.2

DISCLAIMER

This document was prepared as an account of work sponsored by the United States Government. While this document is believed to contain correct information, neither the United States Government nor any agency thereof, nor the Regents of the University of California, nor any of their employees, makes any warranty, express or implied, or assumes any legal responsibility for the accuracy, completeness, or usefulness of any information, apparatus, product, or process disclosed, or represents that its use would not infringe privately owned rights. Reference herein to any specific commercial product, process, or service by its trade name, trademark, manufacturer, or otherwise, does not necessarily constitute or imply its endorsement, recommendation, or favoring by the United States Government or any agency thereof, or the Regents of the University of California. The views and opinions of authors expressed herein do not necessarily state or reflect those of the United States Government or any agency thereof or the Regents of the University of California.

LIFETIME MEASUREMENTS AT PEP AND PETRA*

Gerson Goldhaber**

Lawrence Berkeley Laboratory and Department of Physics
University of California
Berkeley, California 94720

In this talk I will discuss lifetime measurements with various detectors at PEP and PETRA. I will, however, emphasize our own experiment with the SLAC-LBL Mark II detector. This was the first to introduce a vertex detector for more precise lifetime measurements. Subsequently similar devices were introduced in many of the other experiments. In addition, I will also discuss a two-lepton study in the Mark II detector which leads to limits on $B^0\bar{B}^0$ mixing.

1. The Mark II vertex detector

Shortly after the SLAC-LBL Mark II detector moved to PEP a vertex detector⁽¹⁾ was installed. This is a high precision drift chamber which allows one to probe decay lengths in the submillimeter region. This device (see Figure 1) has achieved a resolution comparable or better to the decay lengths being measured.

It is a relatively short cylindrical drift chamber, 1.2 m long, with seven axial layers of drift cells. Four are about 11 cm from the beam line, and three at about 30 cm. To keep multiple scattering to a minimum the chamber has been built directly around a beryllium beam pipe 0.6% of a radiation length thick. The beam pipe serves as the inner gas seal for the chamber. The average resolution per layer in hadronic events is about 100 μ .

A study of the measured distance between the two tracks in Bhabha events after extrapolation to the origin give a distribution of the distance between them of 139 μ which results in a $\sigma \approx 100 \mu$ per track. During three years of operation an integrated luminosity of 220 pb^{-1} was accumulated at $E_{\text{cm}} = 29 \text{ GeV}$ with this chamber.

*This work was supported in part by the Director, Office of Energy Research, Division of High Energy and Nuclear Physics of the U.S. Department of Energy under Contract DE-AC03-76SF00098.

**Miller Professor, Miller Institute for Basic Research in Science, Berkeley, CA 94720. This talk was supported in part by funds from the Nathan Cummings Chair, Tel-Aviv University.

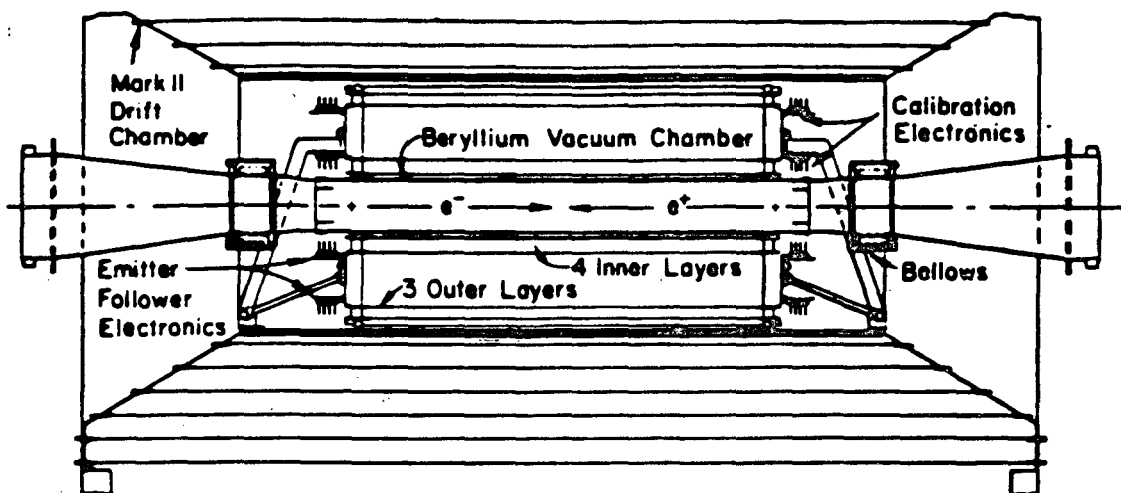


Figure 1

PATH LENGTH ERROR

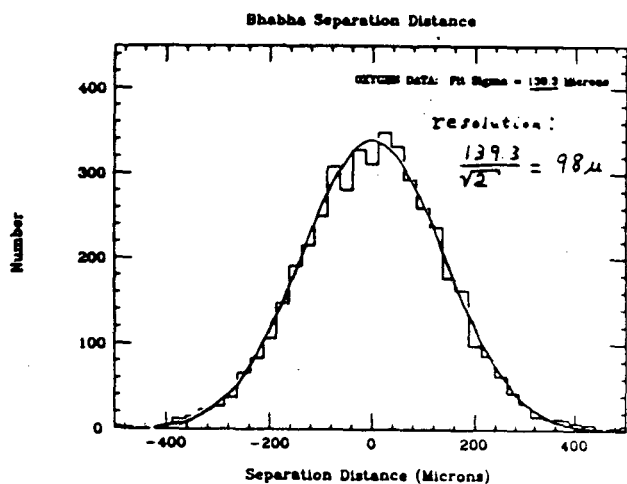


Figure 2

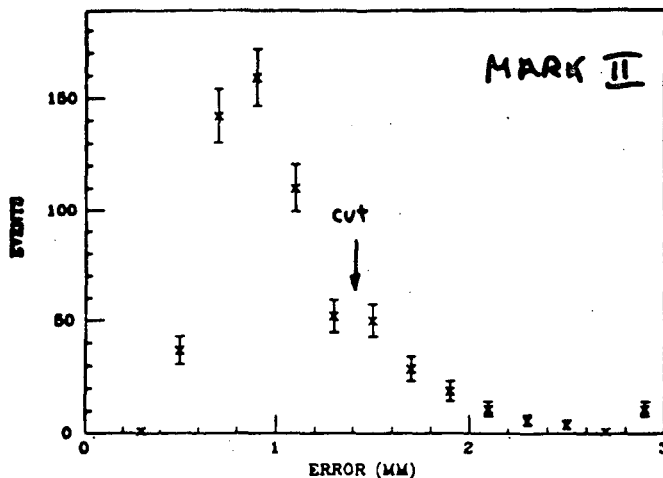


Figure 4

Fig. 1 The Mark II vertex detector.

Fig. 2 Measured distance between two Bhabha tracks. Mark II data.

Fig. 4 Calculated errors in τ decay length. Mark II data.

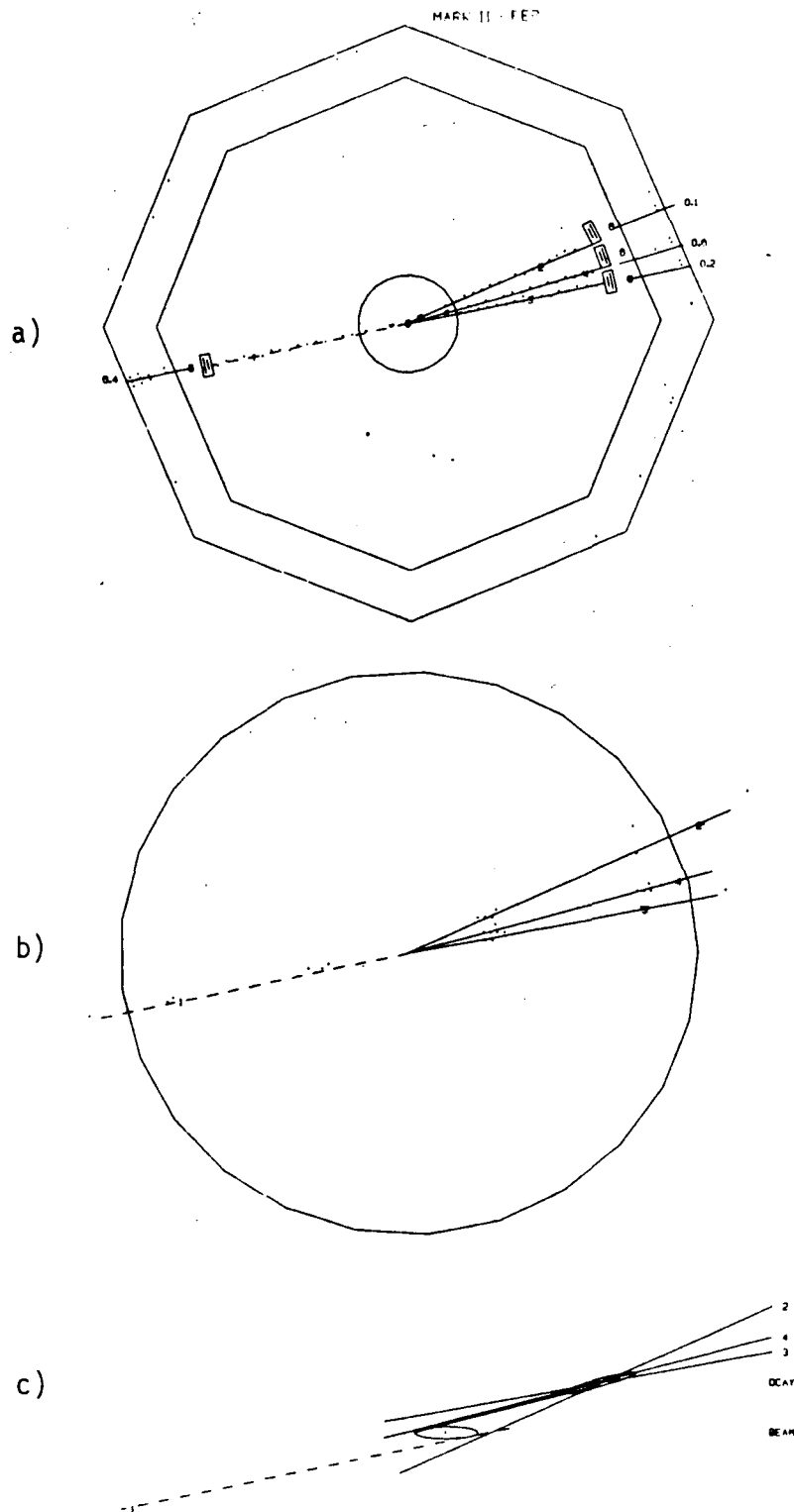


Figure 3

Fig. 3 Example of a $\tau^+\tau^-$ event. Mark II data.

- a) View of the drift chamber, vertex detector and liquid argon shower counters.
- b) View of the vertex detector.
- c) View of the decay vertex. The beam and vertex error ellipses as well as the flight path are also shown. This event corresponds to a 3.0 ± 0.66 mm flight path or 1.2 ± 0.27 psec flight time.

2 The τ lifetime

2.1 Measurements with the Mark II

The τ lifetime provides a sensitive check of the standard model of weak interactions. With the assumption that τ decay proceeds in direct analogy with muon decay, and that the τ neutrino is massless. The tau lifetime can be related to the muon lifetime, namely:

$$\tau_\tau = \tau_\mu \cdot \left(\frac{m_\mu}{m_\tau} \right)^6 \cdot B(\tau \rightarrow e \nu \bar{\nu}).$$

Experimentally

$$B(\tau \rightarrow e \nu \bar{\nu}) = 17.6 \pm 1.1\%,$$

so

$$\tau_\tau = 2.8 \pm 0.2 \times 10^{-13},$$

where the error reflects the uncertainty in the electronic branching ratio.

Furthermore the tau lifetime would be extended if the tau neutrino were massive enough so as to significantly limit the phase space of the decay.

Tau leptons are pair-produced in e^+e^- annihilations, so that each tau has the beam energy. Thus the lifetime can be measured by determining the average decay length of the taus. At PEP with $E_{\text{cm}} = 29 \text{ GeV}$, it is expected to be about 700μ . The decay length can be measured when the tau decays in the three-charged-prong topology. It is the distance between the production point, i.e., the beam position, and the position of the decay vertex.

Events are selected in which at least one of the taus has decayed in the three-charged prong topology and the total charge of the prongs is zero. The three particle invariant mass is required to be in the range $0.7 < m_{3\pi} < 1.5 \text{ GeV}/c^2$, and tau pairs produced by the two-photon process are rejected. Figure 3 shows such an event in the Mark II detector.

The rms beam size at PEP is about 485μ horizontally and 65μ vertically. The average beam position is remarkably stable from one fill to the next. This was measured by finding the average intersection point for an ensemble of well-measured tracks.

The decay vertex position and its error ellipse are determined from the three pion trajectories and their associated errors with a chi-square minimization procedure. Events with a vertex chi-squared per degree of freedom greater than 6 were excluded. The best estimate for the projected decay length l_p is then given in terms of the decay vertex position relative to the beam position, the sum of the beam and vertex error matrices, and the τ direction cosines.⁽²⁾ The tau direction is well approximated by the direction of the 3π system. This measurement is used to transform the projected decay length to the actual decay length in space.

Figure 4 shows the calculated error in the decay length, which depends on the opening angles and orientation of the decay, the tracking errors, and the beam size.

The measured decay lengths are shown in Figure 5, where only those events with decay length errors less than 1.4 mm are included. The mean of the distribution is obviously positive and its shape is asymmetric. The distribution is fitted with a maximum likelihood technique which takes the decay length error into account event-by-event. The fitting function is the convolution of the Gaussian decay length error with an exponential decay distribution. The average decay length is $635 \pm 36 \mu$ for 806 decays.

After correction for hadron contamination and initial state radiation, this yields: $\tau_\tau = (2.86 \pm 0.16 \pm 0.25) \times 10^{-13}$, where the first error is the statistical error and the second is the systematic.

Our latest result is remarkably close to the theoretical estimate. In fact it is the uncertainty in the leptonic branching ratio $B(\tau \rightarrow e\nu\bar{\nu})$ which needs to be improved for a more sensitive search for deviations of experiment from theory!

2.2 Measurements by MAC, DELCO and TASSO

The τ lifetime measurement has become the standard test and calibration for lifetime measurements. The MAC detector has excellent solid angle acceptance and identifies both electrons and muons, but discriminates less well against hadronic backgrounds. Electrons are identified over 72% of the

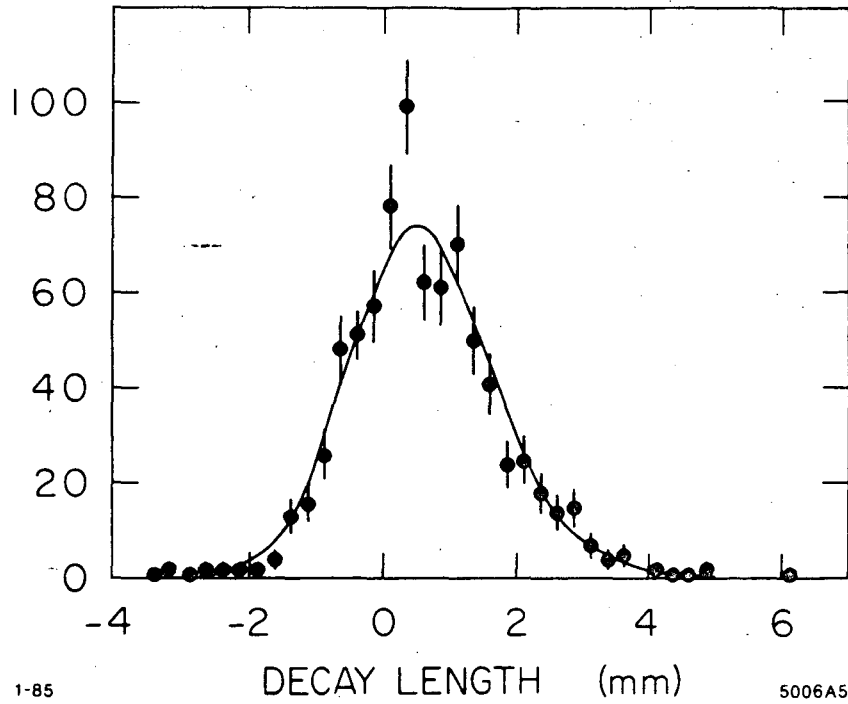


Figure 5

τ WEIGHTED IMPACT PARAMETER

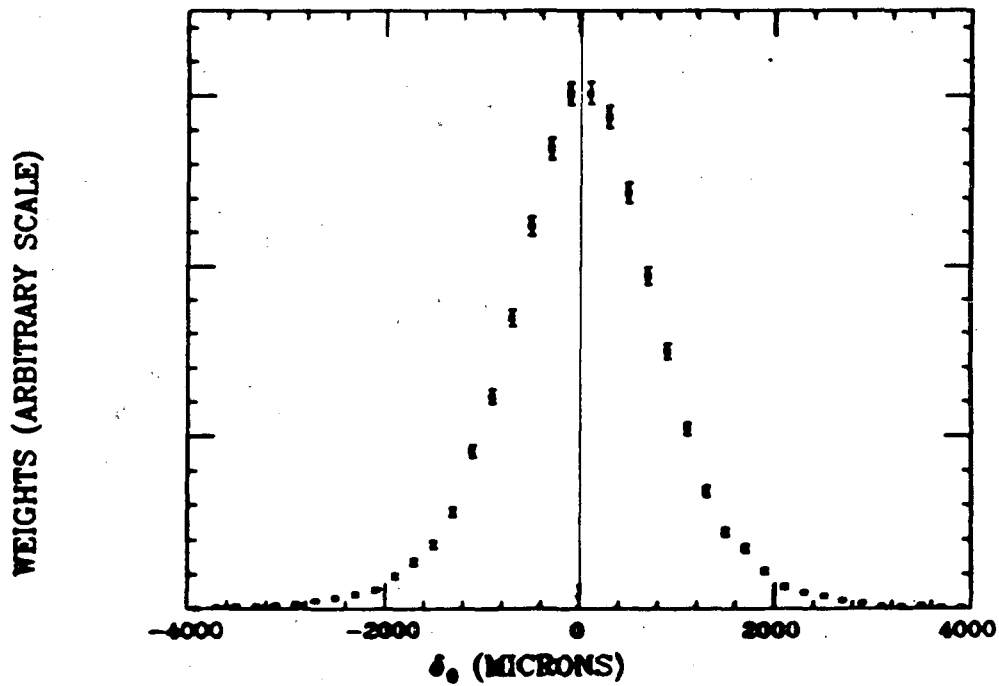


Figure 6

Fig. 5 τ decay length distribution. Mark II data. 806 decay vertices, $\bar{l} = 635 \pm 36 \mu$, $\tau = (2.86 \pm 0.16 \pm 0.25) \times 10^{-13}$ sec.

Fig. 6 Impact parameter distribution for all tracks from τ decay. MAC data. 23,000 tracks, $\bar{\delta} = 46.7 \pm 5.1 \mu$, $\tau = (3.3 \pm 0.4 \pm 0.4) \times 10^{-13}$ sec.

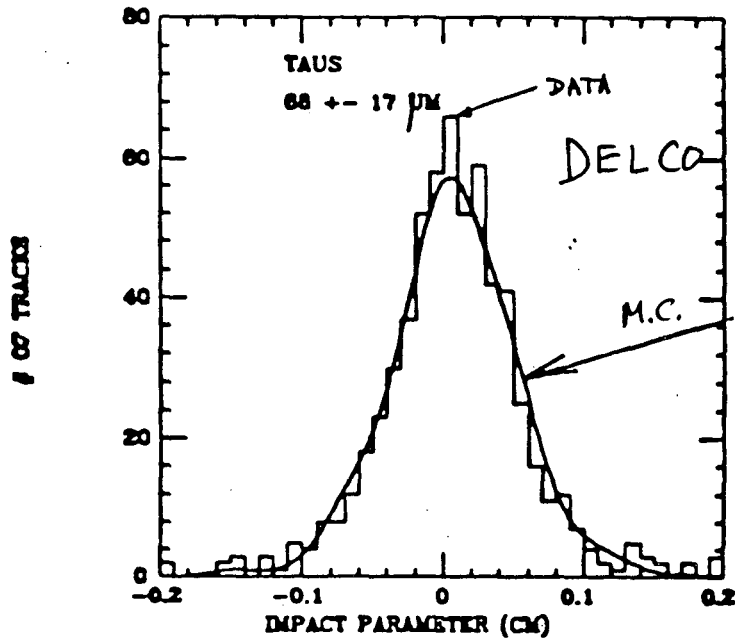


Figure 7

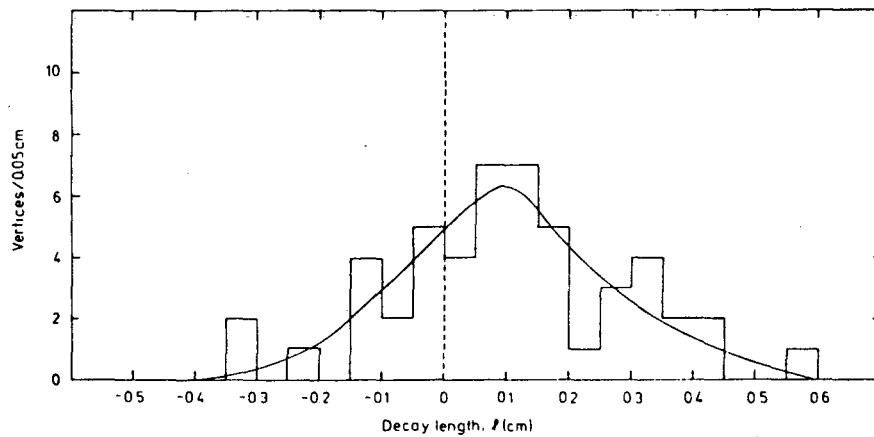


Figure 8

Fig. 7 Impact parameter distribution for tracks from τ decay. DELCO data.

$$\bar{\delta} = 68 \pm 17 \mu, \tau = (2.9 \pm 0.8) \times 10^{-13} \text{ sec.}$$

Fig. 8 τ decay length distribution. TASSO data with vertex detector.

$$48 \text{ decay vertices, } \bar{l} = 1051 \pm 270 \mu,$$

$$\tau = (3.18^{+0.59}_{-0.75} \pm 0.56) \times 10^{-13} \text{ sec.}$$

solid angle by combining charged tracking information with the responses of lead-PWC and iron-PWC calorimeters. Hadronic punch-through is 1/2-1%. Muons are identified by matching tracks which survive the magnetized iron absorber with tracks in the central detector. Between 1-2% of hadronic tracks simulate muons because of punch-through or decay. The MAC central detector has 10 drift chamber layers located between 12 and 45 cm from the beams. This permits modest momentum resolution ($\Delta p/p^2 = 0.065$) and 400 μ extrapolated track resolution for stiff tracks. The DELCO detector is an open geometry magnetic detector with segmented Čerenkov counters and accurate charged particle tracking close to the interaction point. It has a total of 16 drift chamber layers, giving a momentum resolution of $\Delta p/p^2 = .02$ (p in GeV/c). Tracks can be extrapolated to the interaction point with a resolution of 280 μ . Electrons can be identified over 52% of the solid angle with a combination of tracking, Čerenkov and shower counter information. The identification is very clean, thanks to the Čerenkov signal; hadron misidentification is at the 0.1% level. The MAC detector at PEP used "the impact parameter" method⁽³⁾ - for all the tracks in a $\tau^+\tau^-$ events to measure the τ lifetime. See Fig. 6. The DELCO detector also used the impact parameter method⁽³⁾ to measure the τ lifetime - and to test the method for their experiment. See Fig. 7.

The TASSO detector at PETRA has a large drift chamber and solenoid for charged-particle tracking, electromagnetic calorimeters covering about two-thirds of the azimuth, and Čerenkov counters plus shower counters for the remainder. Absorbers and tracking chambers for muon identification are placed beyond the calorimeters in each region. TASSO has recently introduced a vertex detector and measured the τ lifetime by the flight path method for 3 prong τ decays. The higher beam energy, 34 GeV, at PETRA resulted in a longer path length $l = 1051 \pm 270 \mu$ for 48 observed decays. See Fig. 8.

In Fig. 9 I show the summary of all τ lifetime measurements. The first 3 came from Mark II, MAC and CELLO before the introduction of vertex detectors. The mean lifetime, based on the recent measurements, is in excellent agreement with the theoretical value.

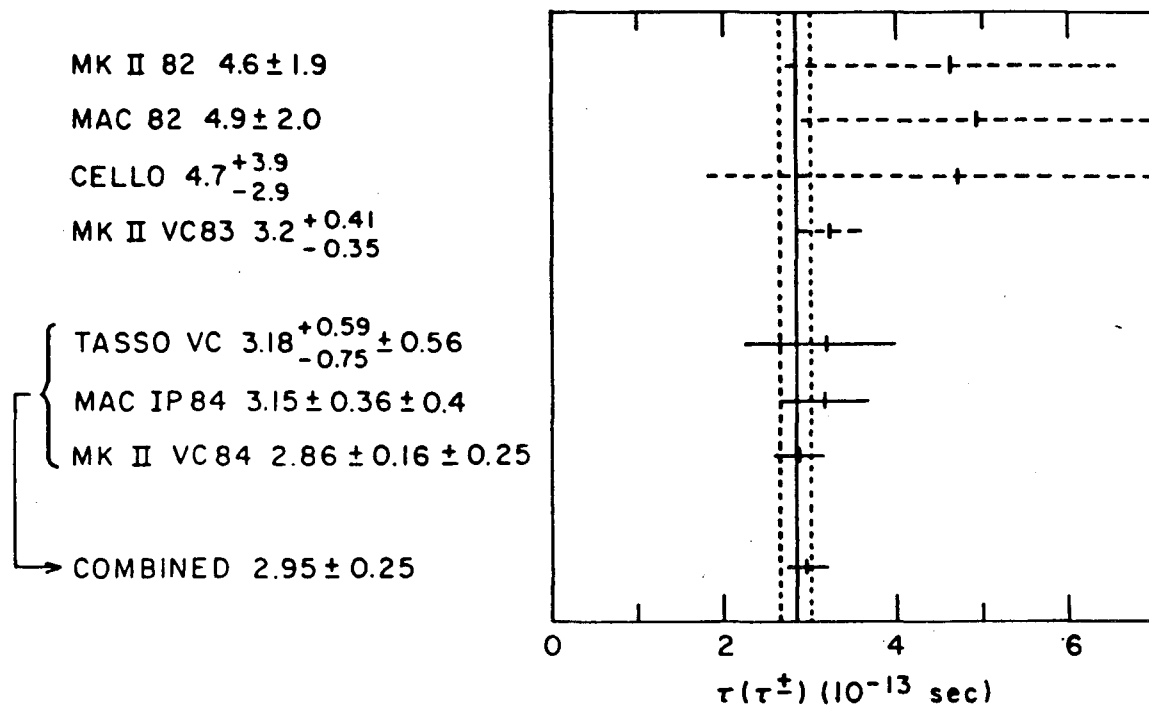


Figure 9

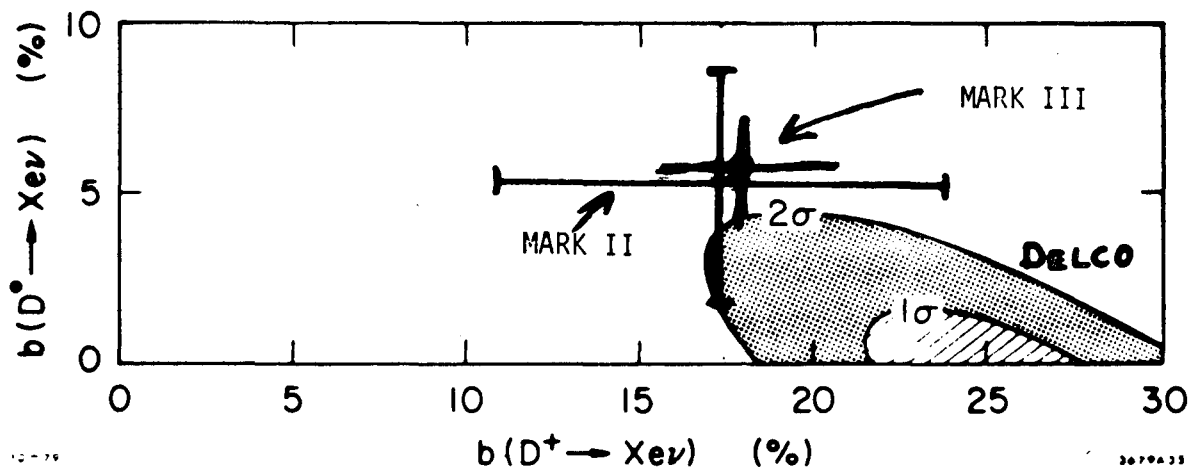


Figure 10

Fig. 9 Summary of τ lifetime measurements. Compiled by W.T. Ford.⁽⁵⁾

The error bars correspond to the statistical and systematic errors added in quadrature. The vertical lines correspond to the theoretical value.

Fig. 10 D^0 vs. D^+ semileptonic branching ratios. Early SPEAR data from MARK II and DELCO as well as recent results from Mark III.

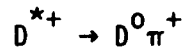
3. Charmed meson lifetimes

It was first noted in 1978 in a measurement of D^+ and D^0 semileptonic branching ratios $B_{\ell}^{+,0}$ that the two lifetimes might be different. If one makes the theoretically reasonable assumption that $\Gamma_{\ell}^+ = \Gamma_{\ell}^0$ where $\Gamma_{\ell}^{+,0}$ are the $D^{+,0}$ semileptonic decay widths then it follows that $\tau^+/\tau^0 = B_{\ell}^+/B_{\ell}^0$. The measurements by the Mark II and DELCO at SPEAR gave $B_{\ell}^+ > B_{\ell}^0$. These results are shown in Fig. 10 together with the more precise recent results from the Mark III at SPEAR⁽⁴⁾.

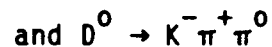
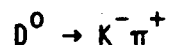
A likely interpretation of these results is that the hadronic decay modes for D^+ and D^0 are different, for example, D^0 decay has additional nonspectator (W-exchange) diagrams available as well as other processes which are currently being investigated in the Mark III experiment at SPEAR. A similar inhibition of a hadronic decay mode is already well known for K^+ decay compared with K_S^0 decay.

3.1 D^0 lifetime Measurement in the Mark II

The sample of D^0 mesons is obtained by observing the decay



with 2 D^0 decay modes



It has previously been shown that this decay can be isolated with very little background at high values of z , where z is the energy of the D^{*+} divided by the beam energy. For the analysis presented here, no attempt to identify particles was made, but all tracks were tried as kaons and pions. All oppositely charged $K\pi$ pairs or $K\pi\pi^0$ triplets respectively with invariant mass between $1.72 \text{ GeV}/c^2$ and $2.00 \text{ GeV}/c^2$ were considered as D^0 candidates and their momenta constrained using the D^0 mass. Each D^0 candidate was then combined with the additional pions of appropriate sign in the event, and those combinations with a small mass difference ($M_{D^0\pi} - M_{D^0}$) and $z > 0.6$ were considered as D^{*+} candidates.

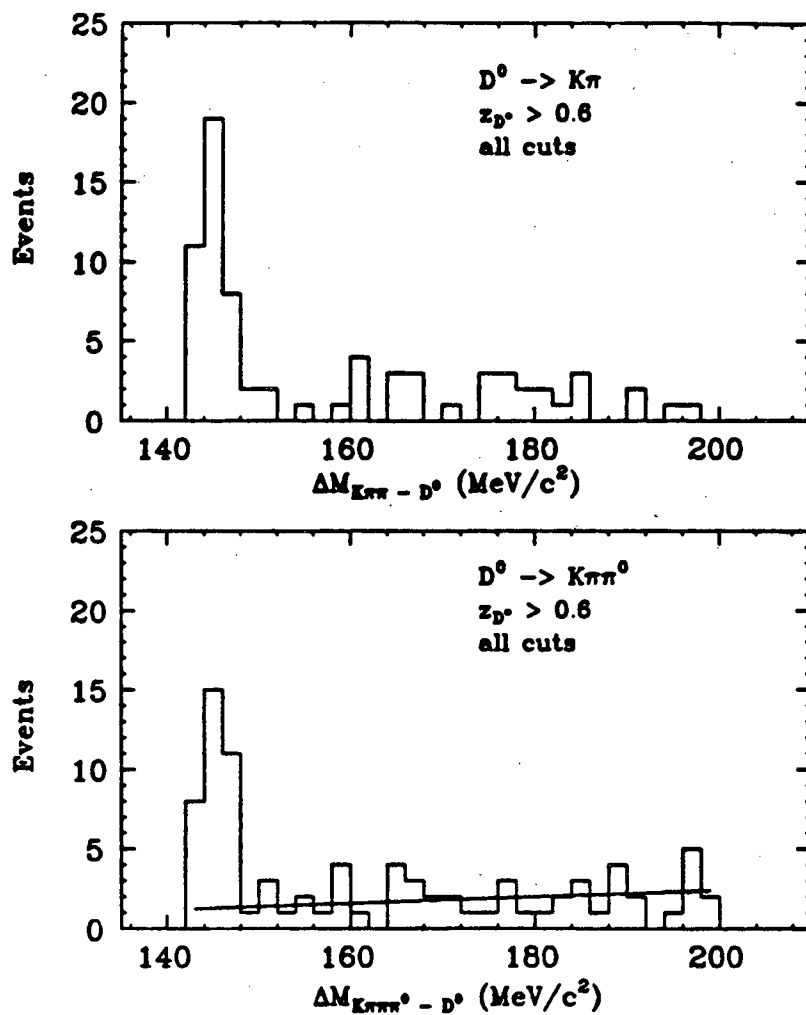


Figure 11

- Fig. 11 a) Mass difference distributions for $D^0 \rightarrow K\pi$ decay.
 b) Mass difference distributions for $D^0 \rightarrow K\pi\pi^0$ decay. Mark II data.

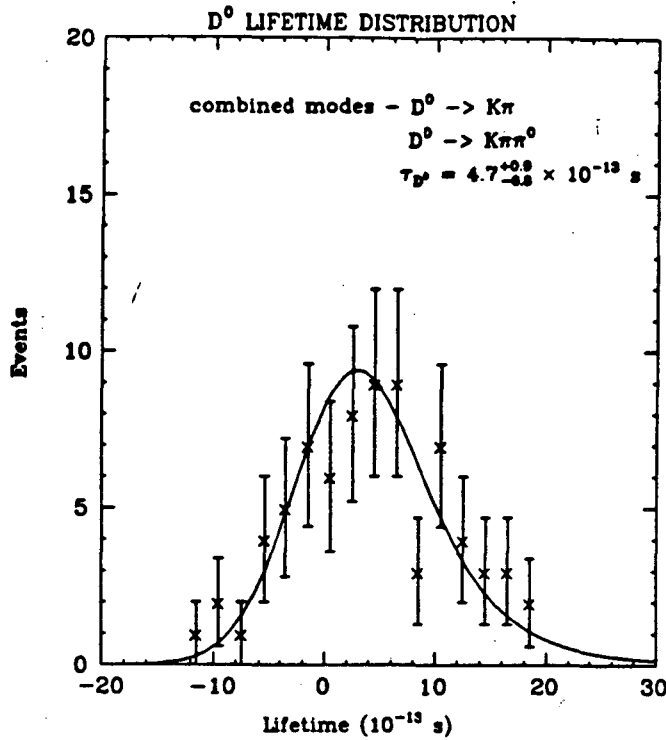


Figure 12

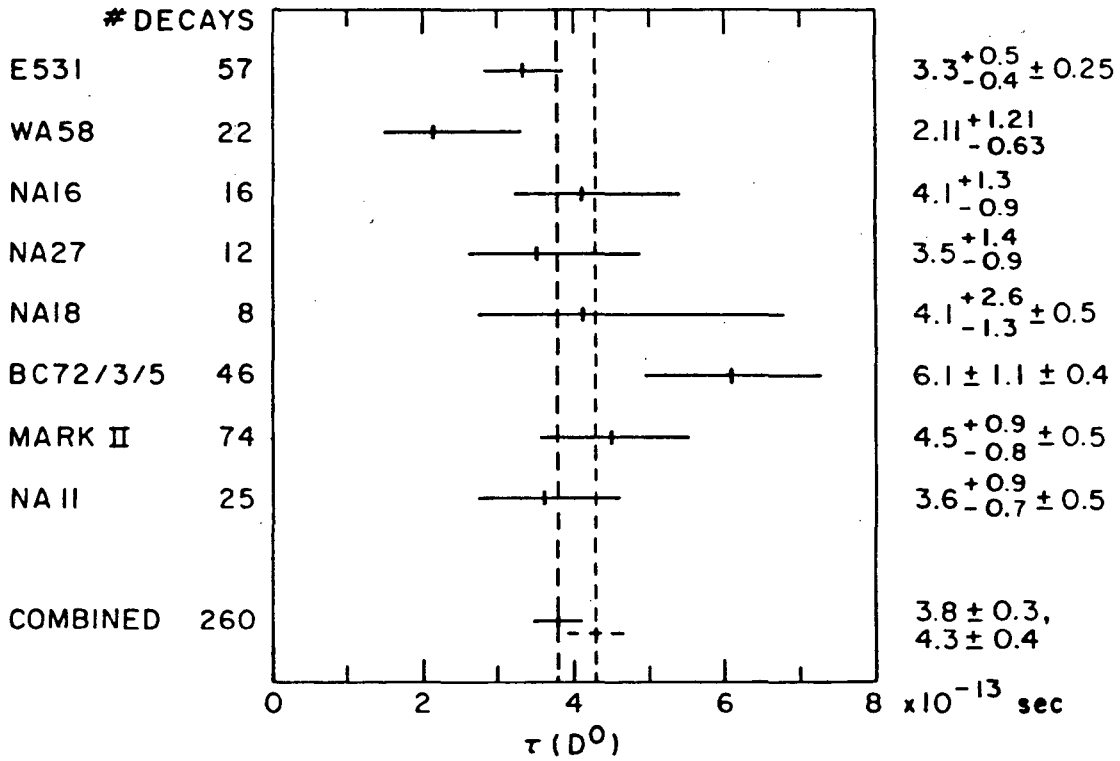


Figure 13

Fig. 12 D⁰ lifetime distribution for all events from the peak regions in Fig. 11 a and b. Mark II data.

Fig. 13 Summary of D⁰ lifetime measurements. "World averages" compiled by W.T. Ford⁽⁵⁾ according to weights: σ^{-2} and $(\sigma/\tau)^{-2}$ respectively.

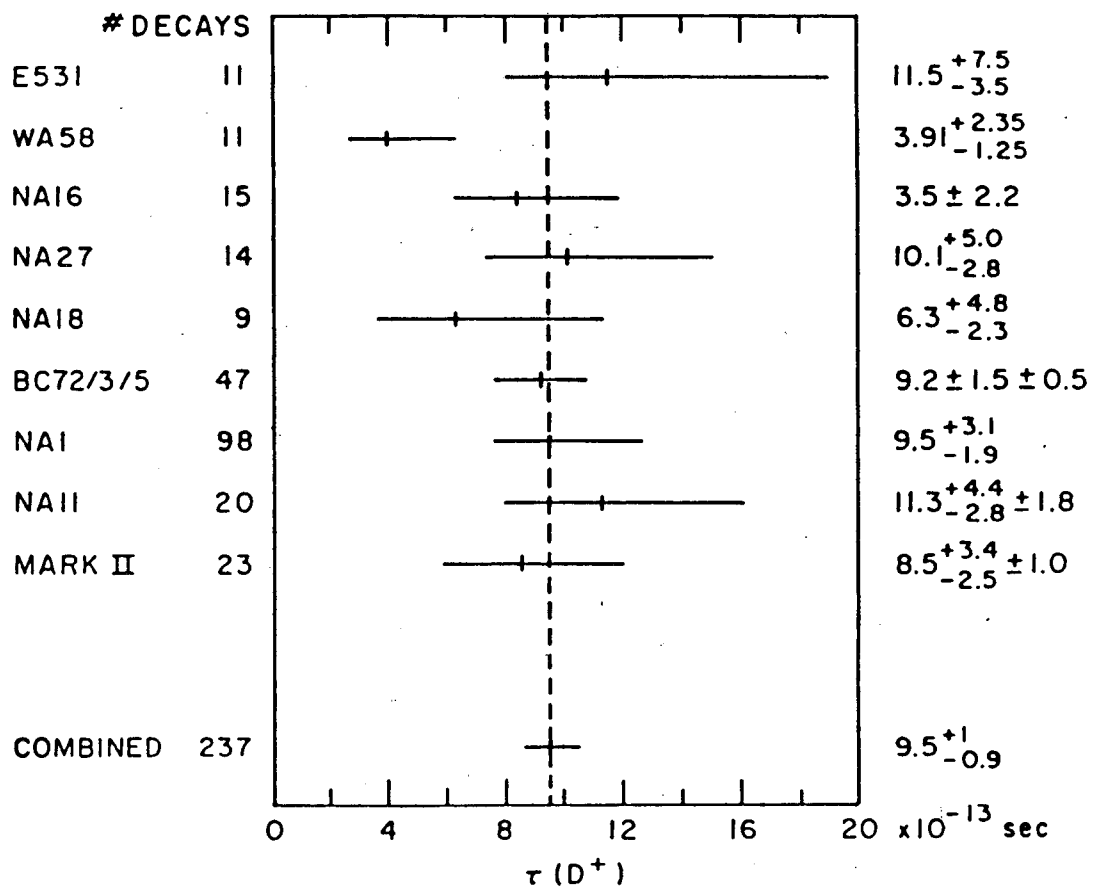


Figure 17

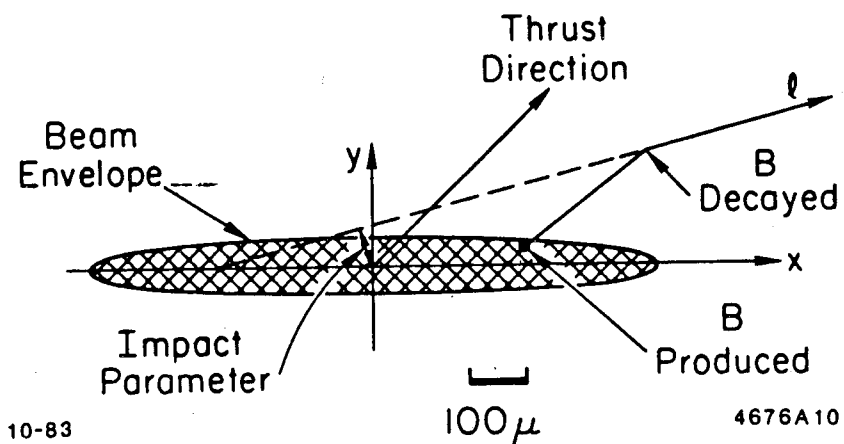


Figure 18

Fig. 17 Summary of D^+ lifetime measurements. (5)

Fig. 18 Sketch of impact parameter.

Further cuts were then applied in order to ensure that the decay point of the D^0 was well measured. To minimize the probability that the K and π tracks from the D^0 had scattered or had suffered tracking confusion, we required that these tracks have momenta greater than 500 MeV/c and no sharing of any vertex chamber measurement points with nearby tracks in the event. The three tracks that made up the D^{*+} were each required to contain at least three measurement points in the vertex chamber, of which at least two were required to be in the inner band of drift cells.

The mass differences after all the cuts are shown in Figure 11a and b for the 2 D^0 decay modes. D^{*+} events were defined to be those with a mass difference between 143 and 149 MeV/c². A total of 39 and 35 events are seen in the two D^{*+} regions and from this figure, the combinatorial hadronic background is estimated to be $12 \pm 6\%$ and $14 \pm 6\%$ respectively. These 74 events were used for the lifetime analysis. In the standard model, B meson decays may contribute up to 20% of the produced D^{*+} events; however, phase space considerations ensure that most of these D^{*+} events are of low momentum, whereas the charm fragmentation function is known to be hard. It is estimated that $3 \pm 2\%$ of the D^{*+} events with $z > 0.6$ originate from B decays.

A histogram of the 74 measurements is displayed in Figure 12. The most probable mean decay time for the D^0 was found by a maximum likelihood fit of the 74 measurements to an exponential decay distribution convoluted with Gaussian errors specific to each event. The fit included effects due to B meson decays and the combinatorial hadronic background as described below. The result of the

fit was a mean decay time of $(4.7^{+0.9}_{-0.8} \pm 0.5) \times 10^{-13}$ s.

We generated a control sample by creating fake D^0 decays out of hadronic tracks having roughly the same kinematics as real D^0 combinations. Tracks which combined with any other opposite charge track in the event to form an invariant mass consistent with that of the K_S^0 were rejected. The mean lifetime of the fake D^0 events was measured to be $(0.4 \pm 0.2) \times 10^{-13}$ s.

Our result is consistent with recent measurements of the D^0 lifetime from other experiments, as shown in Fig. 13.

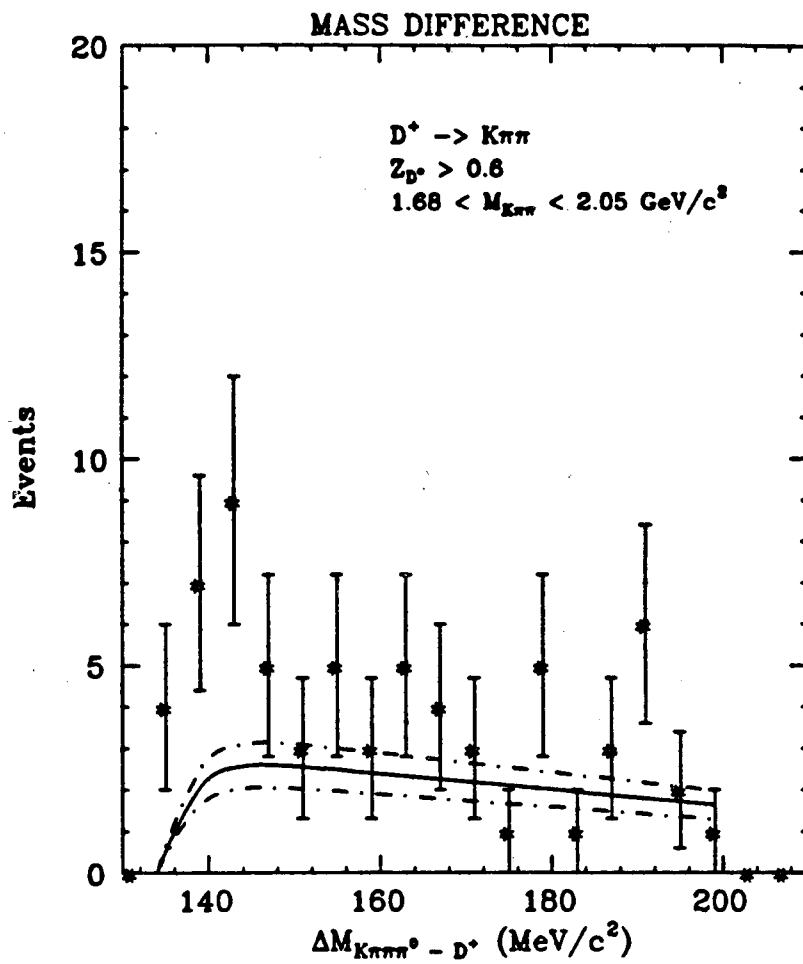


Figure 14

Fig. 14 Mass difference for the D^+ signal region. Mark II data.

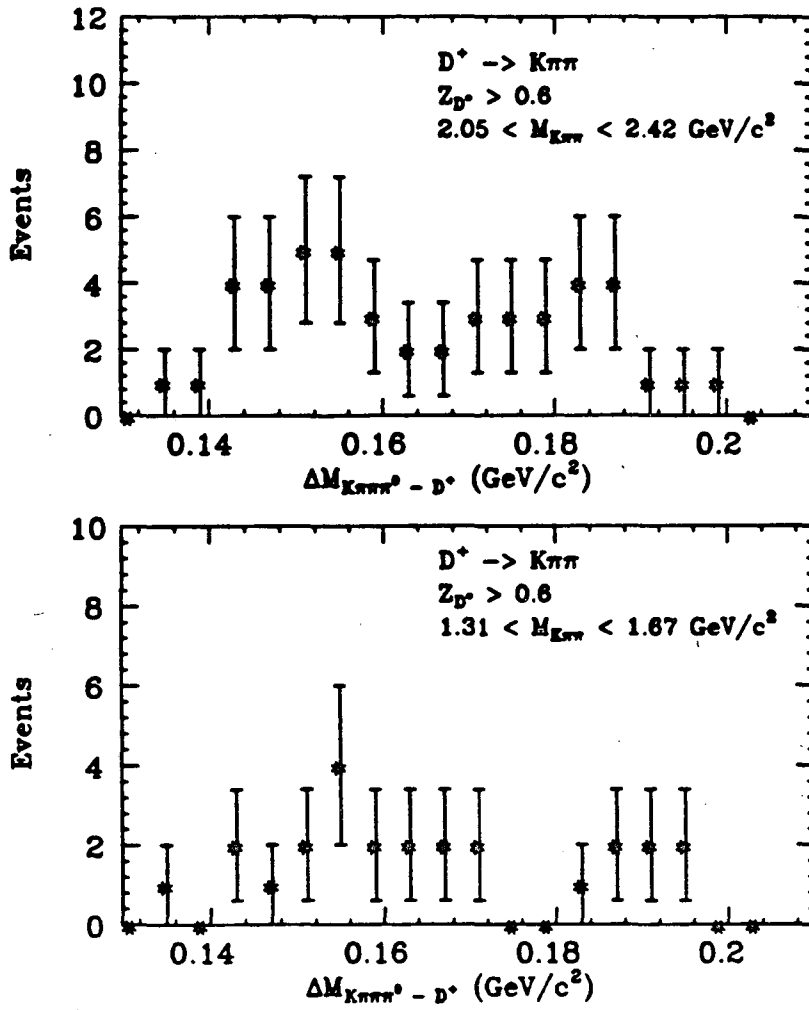


Figure 15

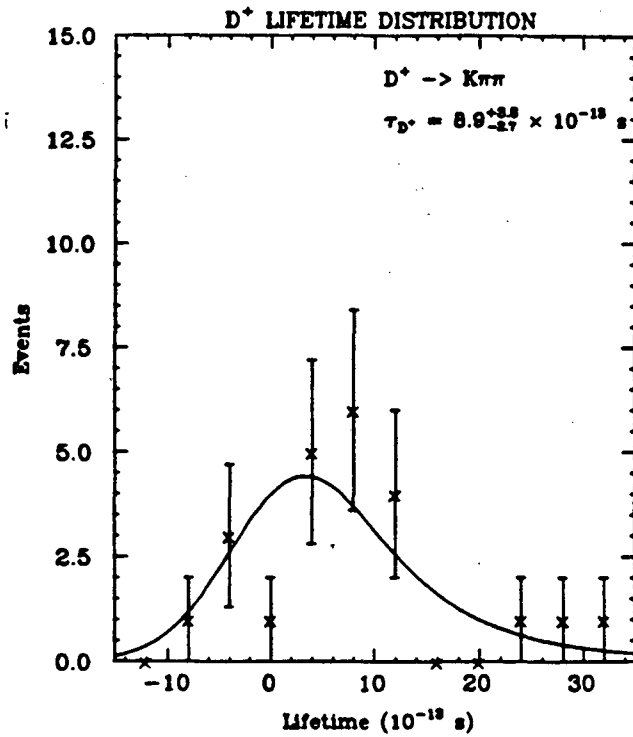


Figure 16

Fig. 15 Mass difference for two D⁺ control regions. Mark II data.

Fig. 16 D⁺ lifetime distribution. Mark II data.

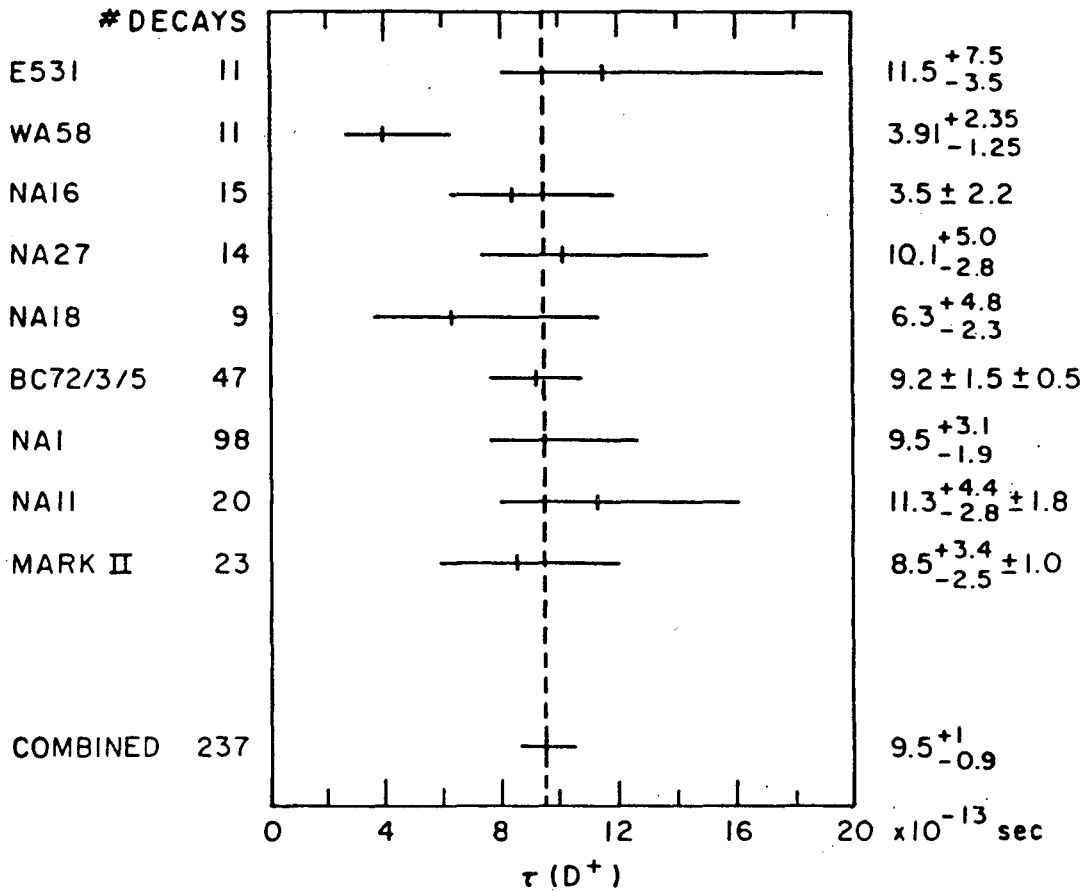


Figure 17

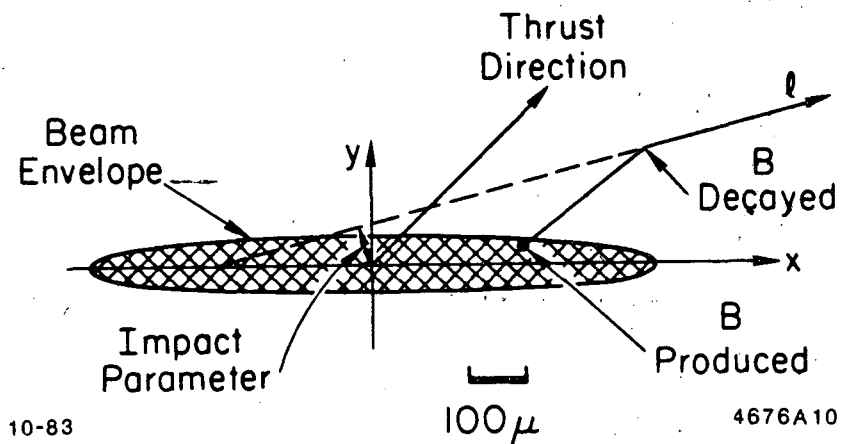


Figure 18

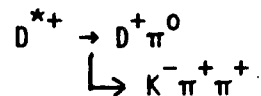
Fig. 17 Summary of D^+ lifetime measurements. (5)

Fig. 18 Sketch of impact parameter.

Very recently the TASSO detector has begun a similar measurement of the D^0 lifetime with the use of their vertex chamber. Preliminary results give: $(4.6^{+2.9+1.0}_{-1.7-1.3}) \times 10^{-13}$ sec based on an exposure of 25 pb^{-1} .

3.2 The D^+ lifetime

D^+ identification in the Mark II detector is more difficult than D^0 identification because here a π^0 is involved in the D^{*+} decay. Aside from that, the procedure used here is quite similar to that described for the D^0 . We locate D^+ mesons via the reaction



where we can again take advantage of the low Q value of the D^{*+} decay to significantly enhance the signal to background ratio.

The mass difference for the signal region in $M_{K\pi\pi}$ is shown in Fig. 14 and for the two control regions in Fig. 15. A mass difference band of 135-146 MeV/c^2 corresponds to the D^{*+} signal. There are 23 events in this band. We estimate 5.7 ± 3.6 of them are due to background, $3 \pm 2\%$ are due to charm from B decays and $14 \pm 6\%$ are attributable to feed through from D^{*0} to $D^0 \pi^0$ decays. The lifetime distribution for the events in the signal band is shown in Fig. 16. After all corrections this yields

$$\tau_{D^+} = (8.9^{+3.8}_{-2.7} \pm 1.3) \times 10^{-13} \text{ s.}$$

This leads to a D^+/D^0 lifetime ratio from the Mark II experiment of $1.9^{+0.9}_{-0.7} \pm 0.3$ which is to be compared to the Mark III D^+/D^0 semi-leptonic branching fraction ratio of

$$2.8^{+0.9+0.3}_{-0.6-0.4}$$

Fig. 17 gives a summary of D^+ lifetimes.

4. Bottom lifetime measurements

The first requirement in measuring B lifetimes is to identify events with hadrons containing b quarks. At the moment we cannot obtain pure samples of such hadrons but rather have to make measurements on "B enriched" samples.

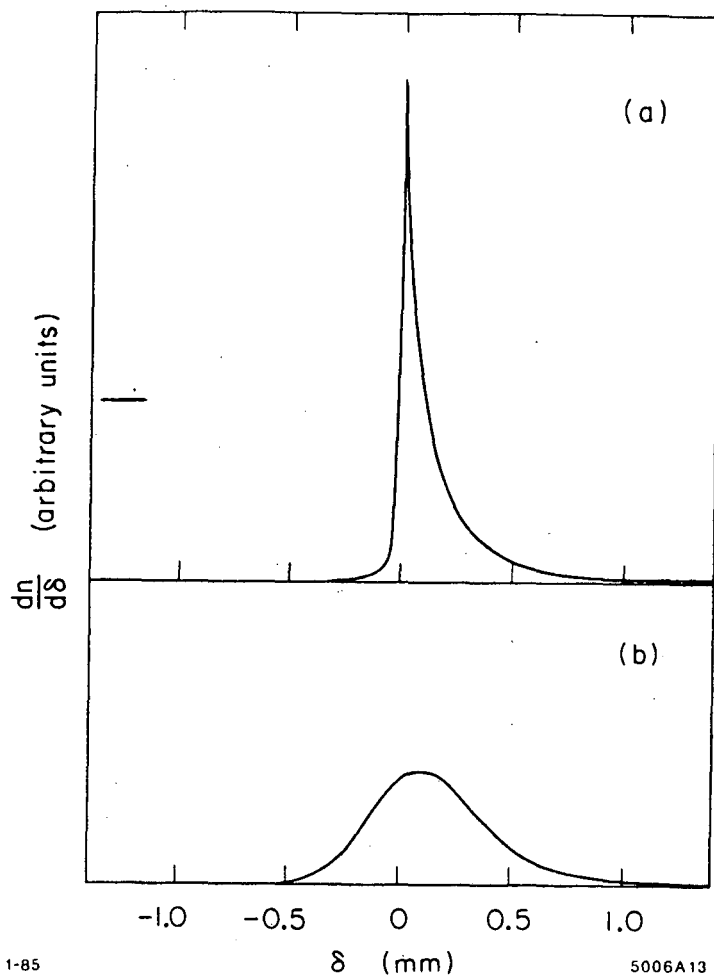


Figure 19

Fig. 19 a) Monte Carlo calculation of impact parameter distribution for 1 psec B lifetime.

b) Distribution as in (a) smeared by measuring error in the Mark II.

Table I

Definition of kinematic regions used for b-enrichment and corresponding b-fraction

DETECTOR	MAC	MARK II	DELCO	JADE	TASSO
b enriched region	$p > 2 \text{ GeV}/c$ $p_T > 1.5 \text{ GeV}/c$	$p > 2 \text{ GeV}/c$ $p_T > 1 \text{ GeV}/c$	$p_T > 1 \text{ GeV}/c$	1.8μ $p > 1.5 e$ $p_T > 0.9$ and anti-3 JET selection	$s_1 \cdot s_2 > 0.1$
fraction of leptons from $b \rightarrow \ell \nu_X$	0.53	0.64	0.77	0.71μ $0.88 e$.32

4.1 The methods for B enrichment

For the Mark II, MAC, DELCO and JADE experiments this B enrichment is obtained by selecting events with identified leptons. The primary sources of leptons in hadronic events are semileptonic charm and B decays after some readily identified events due to the 2 photon processes are eliminated. Other background sources are γ conversion and Dalitz pairs which again can be largely eliminated.

The B enriched versus charm enriched samples can be separated by p and p_T cuts where P_T is the lepton transverse momentum relative to the thrust (or sphericity) axis. Table I shows the P and p_T cuts together with the B fraction achieved with the various detectors.

The TASSO detector used a "topological" method for B enrichment taking advantage of the characteristic event shape of a pair of B decays. B decays give rise to events with high sphericity, however, so do "3-jet" i.e., hard gluon events. To distinguish between these the TASSO group divided the high sphericity events into 2 hemispheres, transformed to the approximate rest frames for each jet and recalculated the two individual jet sphericities S_1 and S_2 . A criterion of $S_1 \cdot S_2 > 0.1$ was then used to obtain a b enriched sample and $S_1 \cdot S_2 < 0.04$ for a b depleted sample. From Monte Carlo calculations it was deduced that the b enriched sample contained 32% $b\bar{b}$, 35% $c\bar{c}$ and 33% light quark pairs.

4.2 B lifetimes from the impact parameter method

The Mark II, MAC, DELCO, and JADE detectors measured the impact parameter δ for the leptons used to obtain the enriched b-samples. Here the thrust (or sphericity) axes were used to define the B direction. Monte Carlo calculations show that this is correct within a few degrees. Here a signed version of the Carlson Hooper and King⁽³⁾ impact parameter method is used. A positive δ value is assigned when the lepton track crosses the thrust axis, or approximate B flight path, which is considered to start at the center of the e^+ beam- e^- beam luminous ellipsoid, so as to correspond to a positive flight path. Otherwise a negative δ value is assigned. Fig. 18 illustrates the impact parameter, Fig. 19 gives a Monte Carlo calculation of the impact parameter distribution for a 1 psec B lifetime for the Mark II

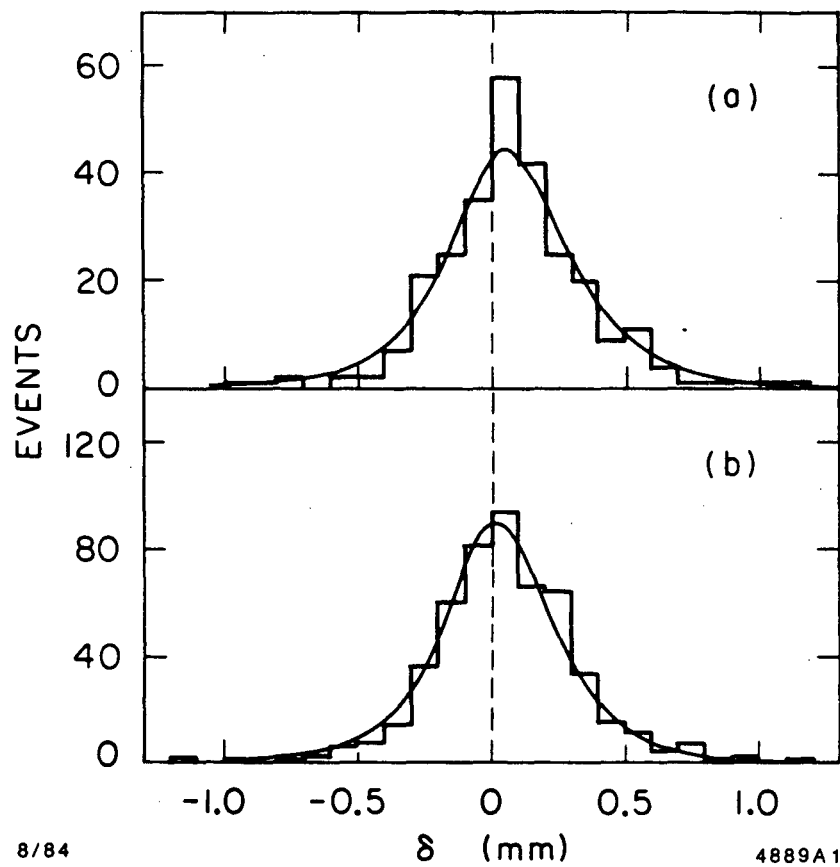


Figure 20

Fig. 20 Impact parameter distribution for the lepton from heavy quark decay.

Mark II data.

a) b enriched region 282 events, $\bar{\delta} = 80 \pm 17\mu$,

$\tau_b = (0.85 \pm 0.15 \pm 0.20)$ psec.

b) c enriched region $\bar{\delta} = 59 \pm 12\mu$.

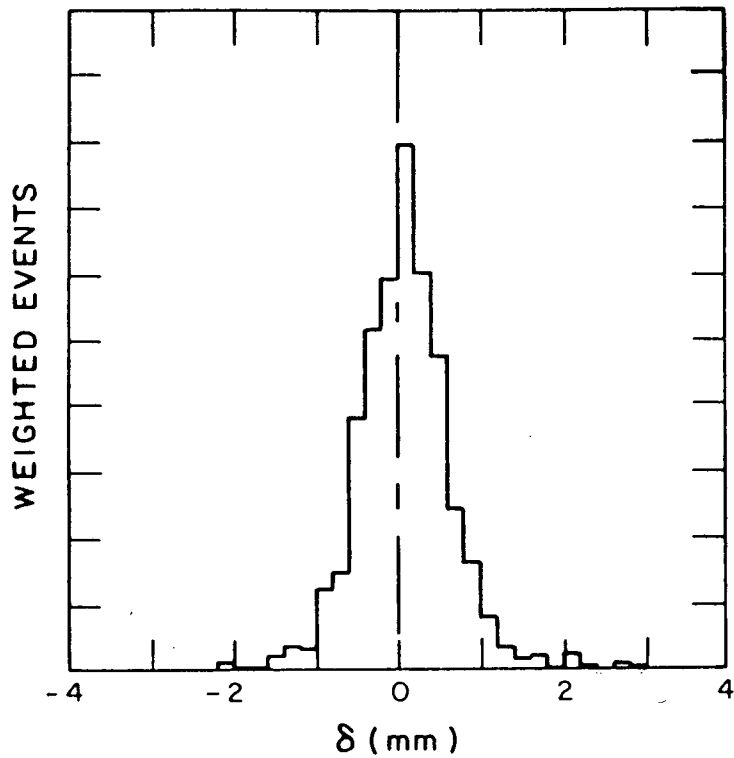


Figure 21

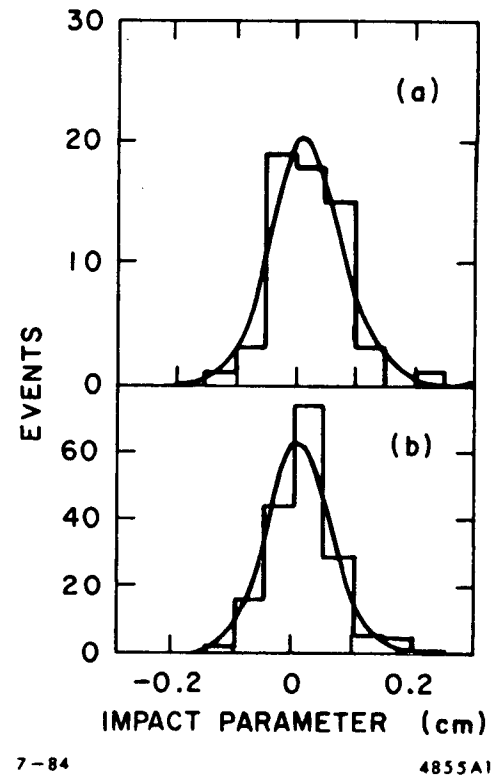


Figure 22

Fig. 21 Updated impact parameter distribution for the lepton in B decay.
 MAC data⁽⁵⁾. 505 events, $\bar{\delta} = 70 \pm 20 \pm 10\mu$,
 $\tau_b = (0.81 \pm 0.28 \pm 0.17)$ psec.

Fig. 22 Impact parameter distribution for the lepton from heavy quark decay.
 DELCO data.

- a) b-enriched region, $\bar{\delta} = 215 \pm 81\mu$,
 $\tau_b = (1.6^{+0.37}_{-0.34} \pm 0.23)$ psec.
- b) Charm enriched region. $\bar{\delta} = 137 \pm 54\mu$.

detector as produced and as smeared by the measurement errors and beam beam vertex position. Figs. 20 to 23 give the updated observed δ distributions for the leptons in the Mark II, MAC, DELCO and JADE detectors.

The TASSO results which correspond to all "good quality" tracks from a given vertex, are given in Figs. 24 and 25. Here they show a comparison of b enriched and depleted data. The earlier data was taken before they introduced their vertex detector while the recent data is taken after their vertex detector was installed.

4.3 B lifetimes by a flight path method

An independent lifetime measurement was used in the Mark II involving the flight path measurement to a reconstructed vertex. The B enriched sample was selected as discussed above from the p and p_T of the observed lepton. A plane perpendicular to the thrust axis was used to divide the event into two jets. A separate vertex is then formed from the well-measured tracks on each side of the event. The distance from each such vertex to the e^+e^- interaction point is determined by a maximum likelihood method. The B lifetime is measured by comparing the distribution of these distances (the "decay length distribution") to distributions obtained from Monte Carlo event samples generated with various B lifetimes. We take the B lifetime to be that lifetime for which the Monte Carlo gives the best fit to the data.

The criteria for "well measured" tracks involve: a momentum cut $p > 600$ MeV/c, cuts on $|z|$ and $|\sqrt{x^2 + y^2}|$ of 5 cm and 5 mm respectively, at least two hits in the 4 inner vertex chamber layers and at least one in the 3 outer layers, and at least 9 hits in the 16 drift chamber layers. Furthermore χ^2 cuts were made on vertex and drift chamber track fits. Finally, tracks which gave two body masses in the K^0 and Λ mass regions were eliminated.

When at least 3 "well measured" tracks were available vertices were constructed for each of the 2 jets per event. This gave two kinds of vertices. Those containing the lepton used in tagging and those without a lepton. In Fig. 26 we show the flight path distribution calculated as for the τ sample for both sets combined.

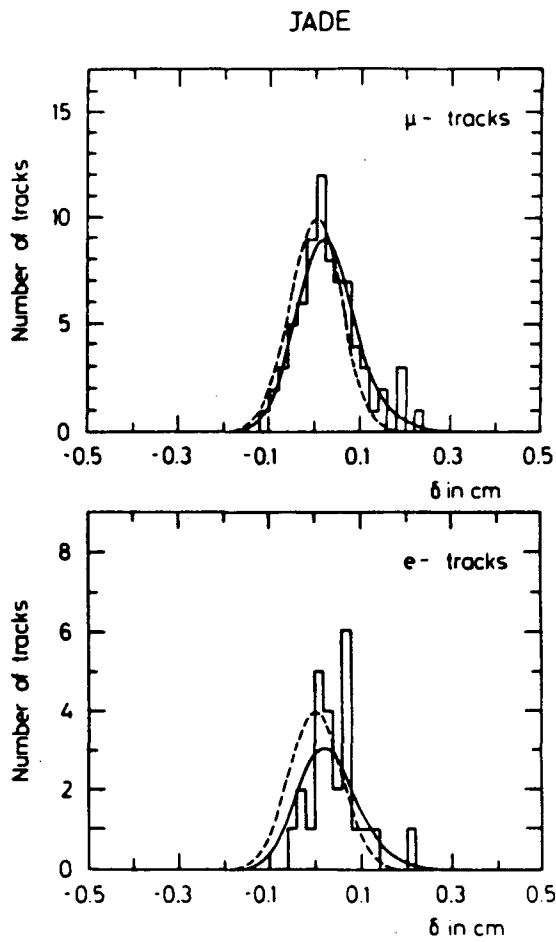


Figure 23

Fig. 23 Impact parameter distribution for the lepton in B decay. JADE data. Muon and electron tracks shown separately for b-enriched region.

$\bar{\delta} = 282 \pm 66\mu$ and $457 \pm 107\mu$ respectively

$\tau_b = (1.8^{+0.5}_{-0.4} \pm 0.4)\text{psec.}$

The dashed curve corresponds to $\tau_b = 0$ and the solid curve to τ_b as measured.

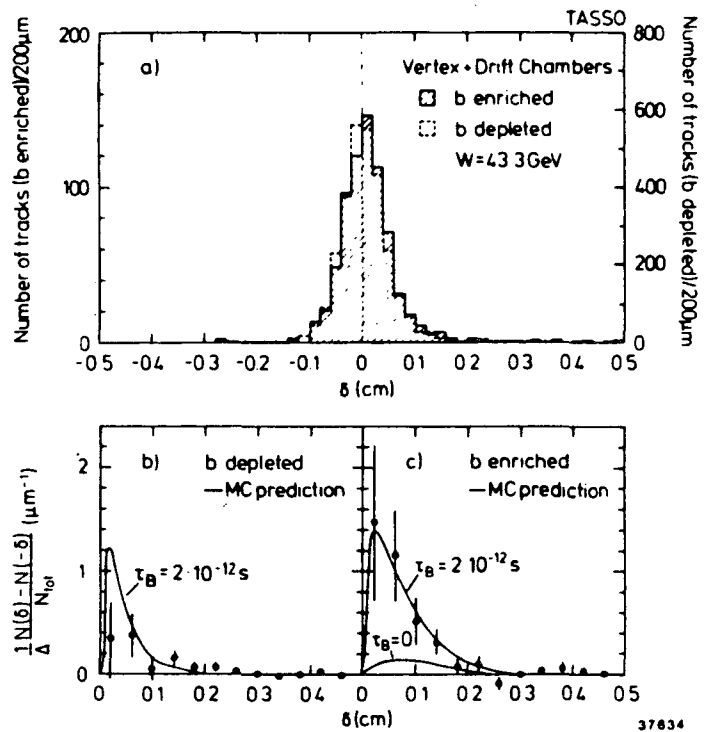


Figure 24

Fig. 24 Impact parameter distribution for all tracks from B decay. TASSO data.

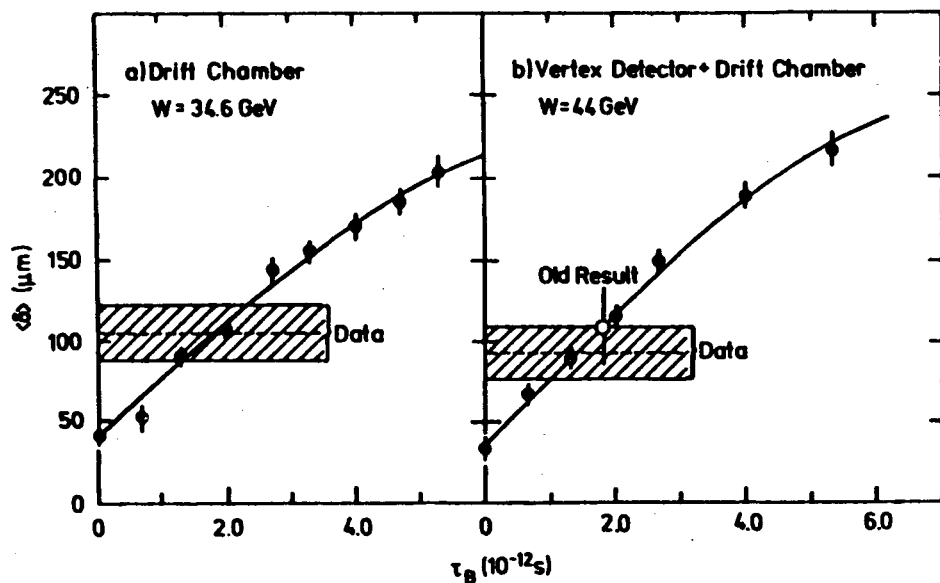


Figure 25

Fig. 25 Lifetime distribution for all tracks from B decay. TASSO data. Curve corresponds to Monte Carlo calculation. Shaded area corresponds to latest measurements. Updated result:
 $\tau_b = (1.57 \pm 0.32)_{-0.34}^{+0.37}$ psec.

Fig. 26 Flight path distribution for B decay vertices. Mark II data.

a) b-enriched region. 551 jets, $\bar{l} = 413 \pm 43 \mu$,

The histogram corresponds to the Monte Carlo fit to the data.

$\tau_b = (1.25_{-0.19}^{+0.26} \pm 0.5)$ psec.

b) c-enriched region. 770 jets, $\bar{l} = 247 \pm 34 \mu$.

c) Random hadrons > 2000 jets, $\bar{l} = 136 \pm 18 \mu$.

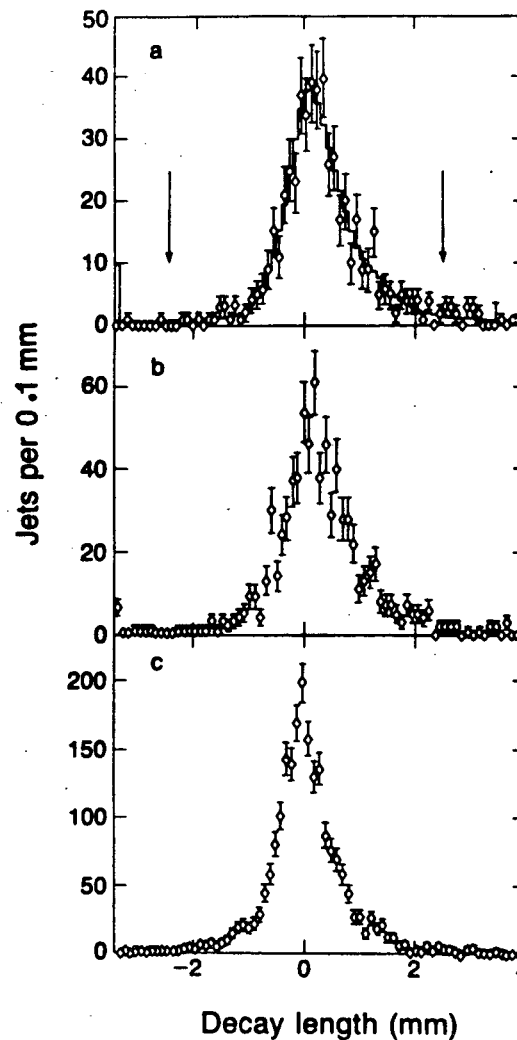


Figure 26

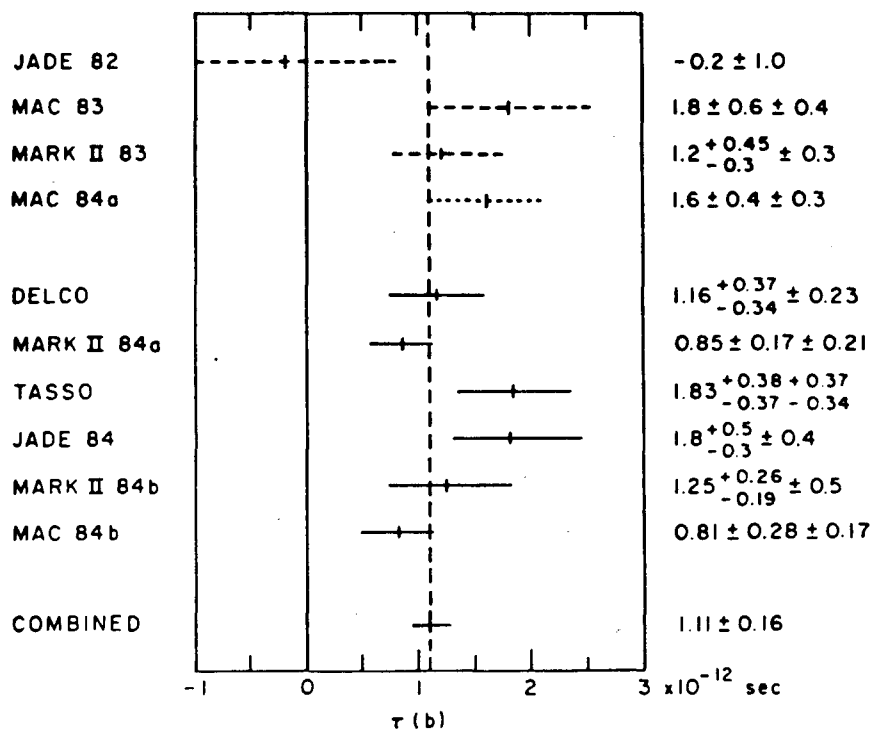


Figure 27

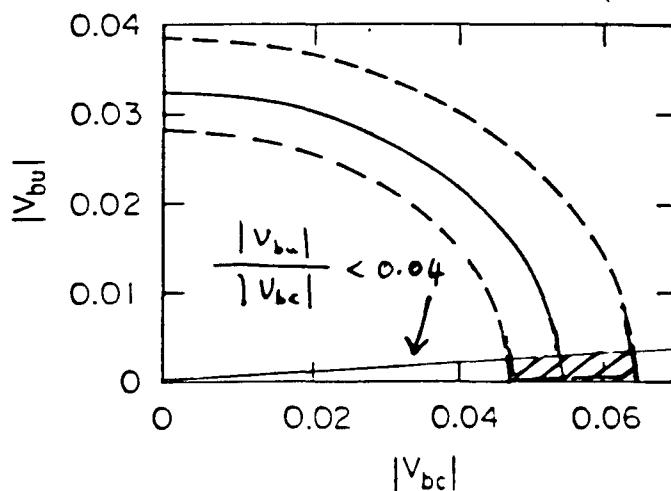


Figure 28

Fig. 27 Summary on B lifetime⁽⁵⁾

Fig. 28 The two Kobayashi Maskawa matrix elements related to b-decay. The lifetime of $\tau_b \approx 1.1$ psec corresponds to the curves shown. The limits of $b \rightarrow u/b \rightarrow c$ semileptonic decays from CLEO, CUSB and recently also ARGUS confine the allowed region of the plane as shown by the shaded part.

Here it must be realized that the tracks selected at each vertex can originate at the beam beam vertex, at the B decay vertex and at the charm decay originating in B decay. To obtain the corresponding B lifetime we rely on Monte Carlo Modeling of the decays. Fig. 27 gives a summary of B decay lifetimes.

4.4 Kobayashi Maskawa matrix elements

The combination of the B lifetime measurement and the study of the semileptonic B decay spectra at CLEO, CUSB and recently also at ARGUS can be used to determine the values⁽⁶⁾ of $|V_{ub}|$ and $|V_{cb}|$. The b lifetime determines a curve in the $|V_{ub}|, |V_{cb}|$ plane. While the direct measurements of the b semileptonic decay give a limit on $|V_{ub}| / |V_{cb}|$ 0.04. Fig. 28 adapted from Klem et. al.⁽⁷⁾ shows the $|V_{ub}|, |V_{cb}|$ plane together with the results of these 2 sets of measurements.

5. Upper limit on $B^0 B^0$ mixing in $e^+ e^-$ annihilation at 29 GeV

With the same criteria for b and c enhancement mentioned above we have also searched for lepton pairs in the Mark II data. Table II shows the experimental distributions of 2 leptons separated into 4 categories: opposite jets and +-, opposite jets and ++ or --, same jet and +-, opposite jets and ++ or --. The predictions, for no $B^0 B^0$ mixing, based on the observed fractions of $b\bar{b}$, $c\bar{c}$ and background is also shown. We determine that the average probability for a semileptonic decay of a hadron initially containing a b quark to produce a positive lepton (wrong sign) is less than 0.12 at the 90% confidence level and set upper limits on $B^0 B^0$ mixing. This limit can be ascribed to $B_d^0 \bar{B}_d^0$ mixing, weighted by the $d\bar{d}$ production probability p_d , and $B_s^0 \bar{B}_s^0$ mixing, weighted by the $s\bar{s}$ production probability p_s , where various cases were considered as shown in Fig. 29. Here r_d and r_s are the ratio of "wrong sign" to "right sign" leptonic B decay for B_d^0 and B_s^0 respectively.

For the assumptions on p_s shown, namely $p_s = 0.1, 0.15$ and 0.2 , our data does not impose a limit on $B_s^0 \bar{B}_s^0$ mixing. If, however, we would assume $p_d = p_u = p_s = 1/3$, what might be considered an upper limit on p_s (see,

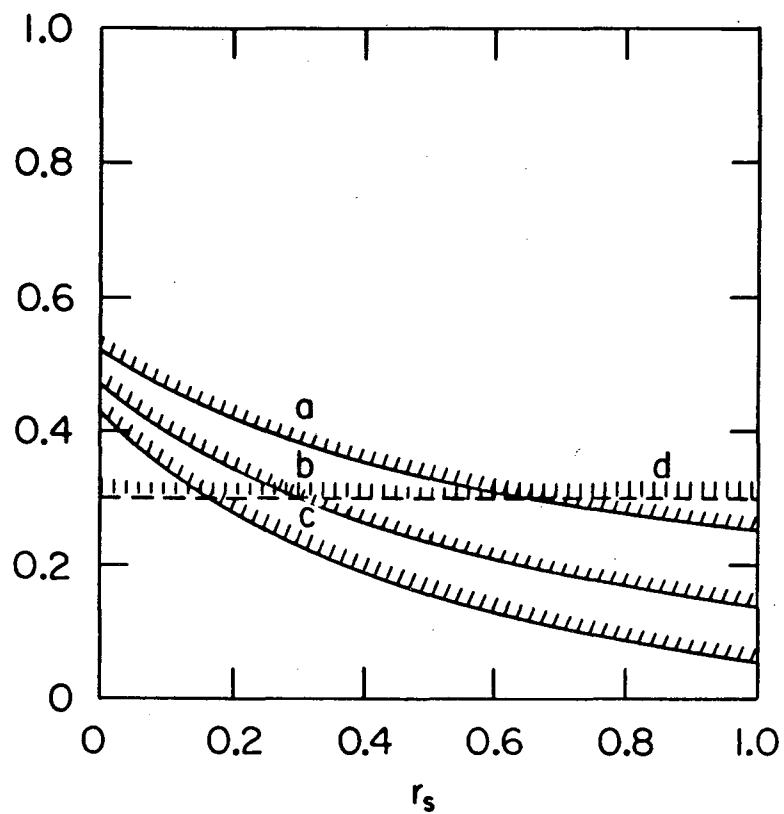


Figure 29

Fig. 29 Limits on $B^0 \bar{B}^0$ mixing. Curves a, b, and c correspond to $p_s = 0.10$, 0.15 and 0.20 respectively from Mark II data. Curve d corresponds to the limit from CLEO data.

A. Ali, this conference) then we begin to impose a mild upper limit on $B_S^0 \bar{B}_S^0$ mixing.

I wish to thank Mrs. Marian Golden and Valerie Heatlie for the careful typing and assembly of this paper.

Table II

Detected (predicted) dilepton events grouped according to kinematic region, jet, and relative charge. The predictions are based on the nominal fractions given in Table I and do not include mixing effects. The quoted errors are estimates of the systematic uncertainties. Mark II data.

Kinematic Regions	Opp. Jet Opp. Sign	Opp. Jet Same Sign	Same Jet Opp. Sign	Same Jet Same Sign
both b -enriched	10 (10.0 ± 2.0)	4 (2.5 ± 0.7)	4 (2.5 ± 0.8)	0 (0.5 ± 0.1)
b -enriched & c -enriched	17 (16.8 ± 5.3)	3 (5.9 ± 1.5)	5 (5.5 ± 1.5)	0 (2.3 ± 0.6)
both c -enriched	13 (11.8 ± 3.2)	2 (4.2 ± 1.0)	4 (3.7 ± 0.9)	2 (2.4 ± 0.6)
Total	40 (38.6 ± 10.3)	9 (12.6 ± 3.2)	13 (11.7 ± 3.1)	2 (5.2 ± 1.3)

References

1. J.A. Jaros, Proc. Int. Conf. on Instrumentation for Colliding Beam Physics, 1982. SLAC Report 250, Ed., W. Ash, p. 174 (unpublished).
2. J.A. Jaros et.al., Phys. Rev. Lett. 51 955(1983).
3. A.G. Carlson, J.E. Hooper and D.T. King, Phil. Mag. 41, 701(1950).
4. R.H. Schindler. Proceedings XXII International Conference on HEP, Leipzig, I, 171(1984). Eds., A. Meyer and E. Wieczorek.
5. W.T. Ford, Aspen Winter Physics Conference, 1985. Ed., M. Block.
6. See for example L.L. Chau, Phys. Reports 95, 1(1983).
7. D.E. Klem, et.al., Phys., Rev. Lett. 53, 1873(1984).

Questions and Comments

W. Reay

Comment: If at any given time one takes the latest results from each group, the D^0 lifetime over several years has been constant at $4.1 - 4.3 \times 10^{-13}$ seconds. Regarding long neutral decays, everyone has a skeleton in the closet. E 531 also had a long decay, less well fit than the SLAC event. Since we never got another, we have simply kept our mouths shut. It would be very interesting for MARK II to search for such long lifetime neutral decays.

G. Goldhaber

We are in the process of carrying out such a search. So far there is no evidence for such long-lived events as the 5.5 psec event observed in the SLAC hybrid bubble chamber experiment.

J. Goldberg

Comment: The lifetime of the unusually long-lived SLAC event (bubble chamber experiment) is not in bad disagreement with the lifetime measured in that particular experiment, but quite far from the "accepted" average.

Question: Would such a long-lived event have been observed in other detectors, such as Mark II, for example?

G. Goldhaber

Yes, I believe so.

A. Bodek

The Mark II number of same sign dimuon events is similar to the UA 1 number. You say that you have no evidence for B^0 mixing, while UA 1 may indicate mixing? Is there a contradiction?

G. Goldhaber

If we use what we consider a reasonable value for p_s we cannot set a limit on $B_S^0 \overline{B_S^0}$ mixing. If we set p_s at 1/3 we get such a limit - it is, however, rather large and hence there is no contradiction.

H. Harari

I seem to remember that the latest Mark II measurement as well as the previous MAC measurement of τ_b gave much larger lifetimes for μ -decay than for e -decay. Is there any explanation for that? Does it happen again at the new MAC experiment?

G. Goldhaber

I think it is a fluke. The updated MAC data has only appeared in a talk at Aspen.⁽⁵⁾ I do not have the corresponding breakdown into e and μ events.

G. Ekspong

When the detector resolution is improved, e.g., by introducing a vertex detector, the lifetimes seem to be shortened. You reported such shortening by factors of about 2 for τ -lepton and for the B-mesons. Is there any reason for systematic errors to influence the measurements such as to cause a lengthening of lifetimes? Can we look forward to still shorter lifetimes for B-mesons?

G. Goldhaber

It does look like a systematic effect. However, by definition we do not understand the systematic errors. Any error we do understand, we correct for. I do think, however, that the B lifetime has settled down to about 1 psec.

This report was done with support from the Department of Energy. Any conclusions or opinions expressed in this report represent solely those of the author(s) and not necessarily those of The Regents of the University of California, the Lawrence Berkeley Laboratory or the Department of Energy.

Reference to a company or product name does not imply approval or recommendation of the product by the University of California or the U.S. Department of Energy to the exclusion of others that may be suitable.

*LAWRENCE BERKELEY LABORATORY
TECHNICAL INFORMATION DEPARTMENT
UNIVERSITY OF CALIFORNIA
BERKELEY, CALIFORNIA 94720*